

## Direct Electron Transfer of Glucose Oxidase in Carbon Paper for Biofuel Cells and Biosensors

Zongqian Hu<sup>1</sup>, Zepeng Kang<sup>2</sup>, Chao Yu<sup>1</sup>, Bing Wang<sup>3</sup>, Shuqiang Jiao<sup>2,\*</sup>, Ruiyun Peng<sup>1,\*</sup>

<sup>1</sup> Beijing Institute of Radiation Medicine, Beijing, 100850, P.R. China.

<sup>2</sup> State Key Laboratory of Advanced Metallurgy, University of Science and Technology Beijing, Beijing, 100083, P.R. China.

<sup>3</sup> Beijing Institute of System Engineering, Beijing, 100101, P.R. China.

\*E-mail: [pengry@bmi.ac.cn](mailto:pengry@bmi.ac.cn), [sjiao@ustb.edu.cn](mailto:sjiao@ustb.edu.cn)

Received: 17 February 2017 / Accepted: 27 May 2017 / Published: 12 July 2017

Advanced bioelectronic devices, such as high-power biofuel cells (BFCs) and highly efficient biosensors, are limited by the difficulty of electron transfer between enzymes and electrodes. Previously reported methods for achieving electron transfer from enzymes to electrodes have relied on the use of complex biomolecule immobilization procedures, complicated matrix materials, or enzyme engineering, resulting in potential relative toxicity, high cost, as well as limited stability. Here, we report a facile method for the rapid preparation of a glucose oxidase (GOx) anode with direct electron transfer (DET) for glucose BFCs and biosensors. GOx is directly incorporated into pretreated carbon paper (CP) by adjusting the pH of the incubation medium during the immobilization process. Excellent bioelectrocatalytic activity is obtained when GOx is incorporated into CP near the pI of GOx. The electron transfer rate constant ( $k_s$ ) and the apparent Michaelis-Menten constant ( $K_M^{app}$ ) are

estimated to be  $12.08 \pm 1.0 \text{ s}^{-1}$  and  $0.13 \pm 0.01 \text{ mM}$ , respectively. These findings may be extended to the development of highly conductive nanomaterials and the immobilization of other enzymes or biomolecules, providing a promising platform for the development of BFCs, biosensors, and other bioelectrochemical devices.

**Keywords:** direct electron transfer; electrostatic adsorption; glucose oxidase; biofuel cells

### 1. INTRODUCTION

With the development of advanced bioelectronic devices, such as high-power biofuel cells (BFCs) and highly efficient biosensors, studies of the direct electrochemistry of redox proteins/enzymes on the electrode surface are becoming increasingly important. In addition to having

practical value, findings from such studies could aid in understanding the fundamental mechanisms of biological redox reactions [1-5]. Owing to its high sensitivity to glucose, glucose oxidase (GOx) has received considerable attention as a potential enzymatic component of BFCs, and for use in real-time glucose monitoring related applications. However, establishing direct electron transfer (DET) between the immobilized GOx and conventional electrodes is a challenge due to the inaccessibility of GOx active centers, which are deeply embedded within a thick insulating protein shell [6,7]. Many attempts at immobilization have been employed to reduce the distance and to improve electron transfer between the active center of GOx and the electrodes [8-11]. These attempts have incorporated various immobilization methods (e.g., physical adsorption [12], cross-linking [13], covalent binding entrapment in gels [14] or membranes [15], self-assembly [16] and layer-by-layer [17] processes), and inorganic/organic matrixes (e.g., metal nanoparticles [18], nanostructured metal oxides [19], carbon nanotubes [10, 20-24], grapheme [25-28], semiconductor nanoparticles [29-32] and conducting polymer nanowires [33]).

Although DET can be achieved on enzyme-modified bioelectrodes, the high cost and complex immobilization procedures for these materials are barriers to their mass commercialization. Therefore, there is great interest in developing a facile procedure enabling enhanced DET to electrodes from immobilized GOx in its natural conformation. Characteristics of the immobilization process, such as pH and temperature, affect the biological activity of the immobilized enzyme and the affinity between the enzyme and the support matrix [34-36]. Differences in the surface charge distribution between an enzyme and a support matrix lead to spatial conformation changes of the enzyme molecule during immobilization [36]. Stanciuc and colleagues recently explored the behavior of enzymes under different pH and temperature conditions, in terms of the relationships among processes, structures, and functions. The enzyme molecule adopted a more flexible conformation under acidic conditions, with the active center being exposed on the molecular surface at optimum pH. Thus, pH treatment can affect the activity and stability of the enzyme molecule [37].

Inspired by previous studies on the behavior of enzymes under different conditions, we developed a facile method for the rapid preparation of a GOx anode with DET for glucose BFCs and biosensors. This method involves adjusting the pH of the incubation medium during the immobilization process. For the support matrix, we used carbon paper (CP) pretreated with a mixed acid solution, which provided good physical and electrical properties and facilitated easy specimen preparation. Using this method, we successfully realized DET from the immobilized GOx to the modified electrode, as well as good bioelectrocatalytic activity for glucose oxidation. The proposed method is highly recommended as a promising platform for advanced bioelectronic device applications.

## 2. EXPERIMENTAL

### 2.1. Reagents and materials

GOx (EC1.1.3.4; from *Aspergillus niger*, ~200 U mg<sup>-1</sup>), D-β-glucose(99.5%), biotin, streptavidin-Cy5, carbon paper (CP), cacodylate, osmium tetroxide, a commercial glucose oxidase

activity assay kit, paraformaldehyde, glutaraldehyde, hexamethyldisilazane, 0.1 M cacodylate buffer (pH 7.4), were supplied from Sigma-Aldrich (St. Louis, MO, USA) and used without further purification. Sodium hydrogen phosphate, sodium dihydrogen phosphate, phosphoric acid (85.11%), nitric acid (65%), sulfuric (98.3%), alcohol(99.8%), calcium chloride (Sinopharm Chemical Reagent Co., Ltd., China) were of analytical grade or better quality and used without further purification. Milli-Q ultrapure water (Millipore,  $\geq 18.2 \text{ M}\Omega \text{ cm}$ ) was used throughout the study.

## 2.2. Preparation of $\text{GOx}_{\text{pH}=\text{x}}/\text{CP}$

CP was used as the support matrix to prepare the modified electrodes. First, CP was cut into a square with an area of  $0.5 \text{ cm}^2$ . To obtain a highly specific surface with a three-dimensional (3D) architecture, the CP square was treated under air for 10 min with a mixed solution of concentrated sulfuric and nitric acids at 3:1 v/v. The resulting pretreated carbon paper sample was washed with abundant Milli-Q ultrapure water until the pH of the wash fluid was neutral. The washed CP was placed in an oven at  $120 \text{ }^\circ\text{C}$  for 1h.

Next, GOx was attached to the pretreated CP ( $\text{GOx}_{\text{pH}=\text{x}}/\text{CP}$ , where x is the pH of the incubation medium). Attachment was achieved by adding  $20 \text{ mg mL}^{-1}$  GOx at various pH values (2, 3, 4, 5, and 7) to the CP and incubating the mixture in a refrigerator overnight. Then, the  $\text{GOx}_{\text{pH}=\text{x}}/\text{CP}$  samples were washed with 0.1 M PBS (pH 7.2). The CP sample with immobilized GOx was stored in PBS (0.1 M, pH 7.2) at  $4 \text{ }^\circ\text{C}$ , and used as the anodic electrode for enzymatic BFCs.

## 2.3. Instruments and Characterizations

The distribution of GOx on the CP surface was studied using confocal laser scanning fluorescence microscopy (PerkinElmer UltraVIEW VoX) and field emission scanning electron microscopy (JSM-6701F, JEOL). In this instance a fluorescent conjugate was used for labeling the  $\text{GOx}_{\text{pH}=\text{x}}/\text{CP}$  (x=2, 3, 7) electrode surface using the covalent bond between the amino groups of GOx and the carboxyl groups of biotin. The background control was performed using the biotinylated fluorescein surface of the CP. The  $\text{GOx}_{\text{pH}=\text{x}}/\text{CP}$  electrode surface was labeled in two steps. An incubation step with  $100 \mu\text{L}$  of biotin/streptavidin-Cy5 solution (10 mM of biotin and  $0.02 \text{ mg mL}^{-1}$  of streptavidin-Cy5 fluorescent dye) in PBS (0.1 M, pH 7.2) at  $25 \pm 2 \text{ }^\circ\text{C}$  during 60 min was performed. After that, three washing steps with PBS (0.1 M, pH 7.2) at  $25 \pm 2 \text{ }^\circ\text{C}$  during 5 min were performed [38].

In preparation for FESEM of the  $\text{GOx}_{\text{pH}=\text{x}}/\text{CP}$  (x=2, 3, 7), the samples were fixed overnight at  $4 \text{ }^\circ\text{C}$  in 20 volumes of modified Karnovsky's fixative (2% paraformaldehyde, 2.5% glutaraldehyde, 1.7 mM  $\text{CaCl}_2$  in 0.1 M cacodylate buffer, pH 7.4). The fixed samples were washed twice in 0.1 M cacodylate buffer (pH 7.4) and postfixed in osmium solution (1% osmium tetroxide in 0.1 M cacodylate buffer) overnight at  $4 \text{ }^\circ\text{C}$ . The samples were washed twice with double-distilled water, dehydrated in ascending grades of alcohol (30%, 50%, 70%, 95%, and 100%), treated for 5 min with hexamethyldisilazane (Electron Microscopy Supplies, Ft. Washington, PA), dried, and sputter coated

with gold (ISMSCD-2, sputter coater device). As a control, the bare CP and pretreated CP were treated using the same procedures.

Zeta potentials of pretreated CP in PBS at various pH values were characterized by dynamic light scattering on a Zeta Sizer Nano ZS instrument (Powereach, JS94H, Shanghai). A CHI 660E workstation was used to collect electrochemical data. All experiments were conducted at  $25 \pm 2$  °C with a conventional three-electrode system under the cyclic voltammetry (CV) cycle, electrochemical impedance spectroscopy (EIS) and chronoamperometry (CA). Electrodes included the prepared electrode as the working electrode, a platinum sheet with a surface area of  $2 \text{ cm}^2$  as the counter electrode, and Ag/AgCl (3 M KCl) as the reference electrode. Except in the pH-dependent experiments, 0.1 M PBS (pH 7.2) was employed as the supporting electrolyte.

Only  $\beta$ -D-glucose acts as a substrate for the enzymatic reaction with GOx. Therefore, the glucose stock solution (prepared in PBS) was subjected to mutarotation at 4 °C for at least 24 h before use. Before the CV experiments were performed, the electrolyte was deoxygenated by bubbling highly purified argon through the solution at least 30 min. An argon atmosphere was maintained over the solution during the electrochemical measurements. The apparent Michaelis-Menten constant ( $K_M^{app}$ ) of GOx was measured by the chronoamperometric  $i$ - $t$  response. Aliquots of  $\beta$ -D-glucose stock solution were added into 30 mL of stirred PBS in an electrochemical cell. The mean value of the anodic current (in  $\mu\text{A}$ ) was plotted against the  $\beta$ -D-glucose concentration (in mM).

#### 2.4. Design and testing of the BFC

To maximize the bioelectrocatalytic activity of the prepared bioanode, a hybrid BFC design was employed. This design consisted of the  $\text{GOx}_{\text{pH}=x}/\text{CP}$  anode and an air-breathing Pt cathode. The anode fuel reservoir and the cathode holder of the cell were connected with a salt bridge. The anode fuel reservoir was operated at room temperature and fed with a fuel solution of  $\beta$ -D-glucose stock solution (0.1 M, pH 7.2) under highly purified saturated argon. A  $2 \text{ cm}^2$  platinum sheet, used as the cathode, was placed in Britton-Robinson buffer solution (B-R buffer solution, pH 3, prepared with equimolar of 0.04 M phosphoric acid, boric acid and acetic acid; the pH was adjusted with 0.2 M NaOH solution) under highly purified saturated oxygen. To minimize the negative impact of the cathode on the overall performance of the BFC, the working temperature of the Pt cathode was increased to  $90 \pm 10$  °C. The current density and power density of the BFC were calculated using data from the polarization curve.

### 3. RESULTS AND DISCUSSION

#### 3.1. Surface characteristics of $\text{GOx}_{\text{pH}=x}/\text{CP}$

Figure S1 shows the FESEM images of bare CP and pretreated CP before enzyme immobilization. Whereas the bare CP surface appears smooth and compact, the pretreated CP surface is composed of multiple thin, stacked, and laminated sheets connected to each other. The pretreated CP,

with its larger specific area and 3D structure, can potentially be used as a support matrix for GOx immobilization.

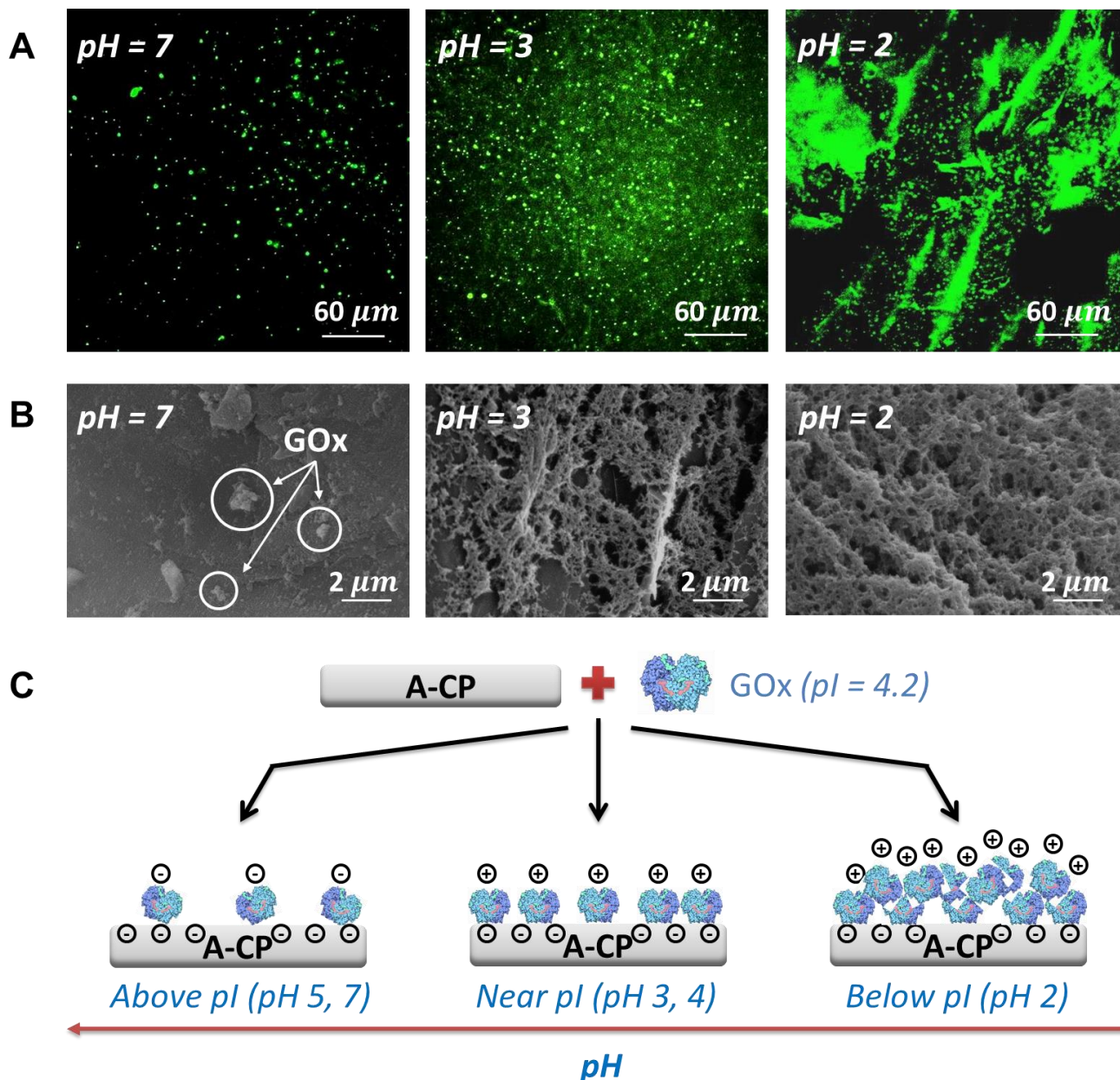


**Figure 1.** (A) Confocal laser scanning fluorescence microphotograph for the  $GOx_{pH=2, 3, 7}/CP$ . The laser excitation is at 640 nm and the voltage is 360 V. (B) FESEM images of the surface of the  $GOx_{pH=2, 3, 7}/CP$ . (C) Schematic representation on the effect of pH on the adsorption of GOx in CP. The isoelectric point (pI) of GOx is 4.2, where the protein net charge is expected to be neutral [39], above this value, for example, at a pH of 5 and 7, it is negative, and below this value, is positive (i.e. 4, 3 and 2).

Confocal laser scanning fluorescence microscopy and FESEM were used to evaluate the distribution of the GOx on the CP surface at various pH values. As shown in Figure 1A, the intense fluorescence area of the  $GOx_{pH=x}/CP$  increases with the decrease of the pH from 7 to 2. The intense

fluorescence area corresponds to GOx bonding with the fluorescent marker. It indicates that the distribution of GOx on the CP surface under acidic conditions is much greater than that under neutral conditions. The FESEM images of the  $\text{GOx}_{\text{pH}=x}/\text{CP}$  also indicate that GOx adsorbed on the CP surface with different aggregate morphologies depends on the pH of the incubation medium (Figure 1B), and the adsorption of the immobilized GOx increases with decreasing pH of the incubation medium.

These differences in distribution and morphology may be related to the surface charge distribution between the GOx molecules and the CP [39]. The isoelectric point (pI) of GOx is 4.2 whereas the protein net charge is expected to be neutral, while above this value, for example at a pH of 5 and 7, it is negative, and below this value, it is positive (i.e. 4, 3 and 2) [39]. Zeta potentials of the CP surface in the GOx solution at all tested pH values are negative (Table S1). Considering this fact it can be argued that since at a pH of 4, 3 and 2, where the GOx molecules are positively charged, a higher adsorption is expected to occur. This is due to an increase in the hydrophobic interactions and attractive forces between GOx (positive) and the pretreated CP surface (negative), creating a highly packed GOx layer on the CP surface resulting in higher adsorption, see Figure 1C. However, a thick layer of GOx film was formed on the CP surface when the pH was very low (pH 2; Figure 1A and Figure 1B). This thick insulating layer of GOx hinders electron transfer from the GOx active center to the electrode surface. The results from the FESEM are consistent with those from confocal laser scanning fluorescence microscopy.

### 3.2. DET of $\text{GOx}_{\text{pH}=x}/\text{CP}$

The direct electrochemical catalysis reaction of flavin adenine dinucleotide (FAD/FADH<sub>2</sub>) is a crucial symbol of DET between GOx and the electrodes as well as for the cofactors that are the main places to complete the redox reaction where two electrons and two protons are transferred [40]. The reaction mechanism is shown in formula (I):



Therefore, the electrochemical behaviors of different  $\text{GOx}_{\text{pH}=x}/\text{CP}$  samples were investigated. As shown in Figure 2, a pair of distinct and symmetric redox peaks is observed for all samples except  $\text{GOx}_{\text{pH}=7}/\text{CP}$ . The redox peak current density of GOx/CP increases with the decrease of the pH. The formal potential ( $E^0$ ) is determined as the average of the cathodic and anodic peak potentials. The  $E^0$  values are -0.47, -0.45, -0.46, and -0.46 V at pH values of 2, 3, 4, and 5, respectively. Our results are consistent with those reported in the literature for the reversible reaction of FAD within GOx [29, 41]. This observation demonstrates the successful immobilization of GOx on the electrode surface and the achievement of good electrical coupling between the enzyme and the electrode. However, the CV curve of  $\text{GOx}_{\text{pH}=2}/\text{CP}$  shows a very wide peak separation between the anodic and cathodic peaks ( $\Delta E_p$ , 378 mV), indicating weak protein adsorption properties and sluggish electron transfer.

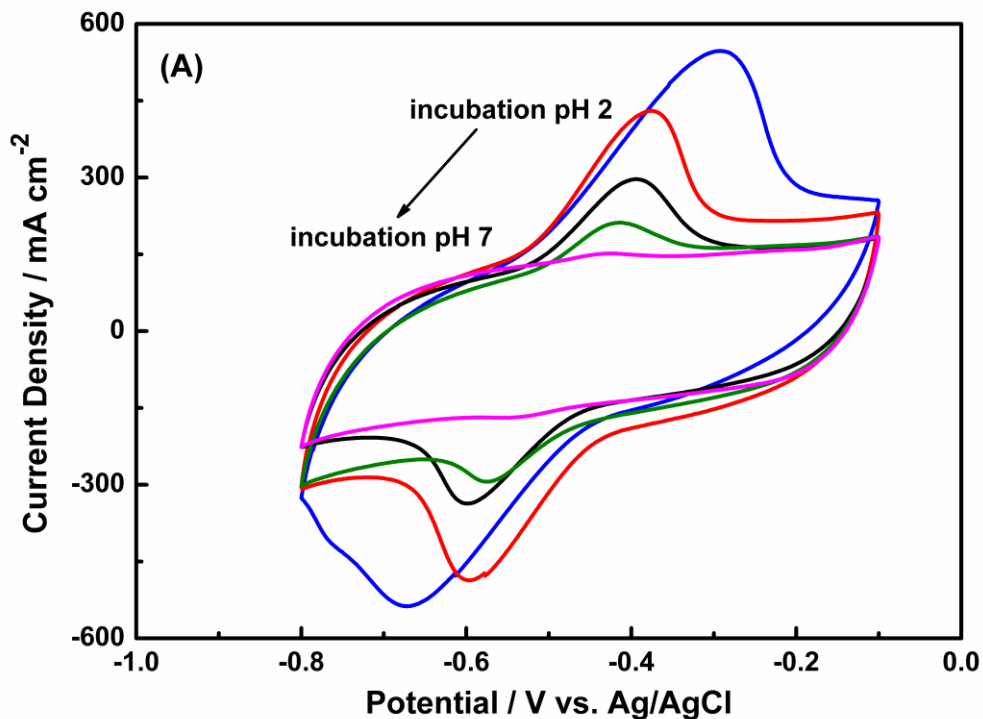


**Figure 2.** CVs of the  $GOx_{pH=2,3,4,5,7}/CP$  in  $O_2$ -free 0.1 M PBS (pH 7.2) with the potential scan rate is  $10 \text{ mV s}^{-1}$ .

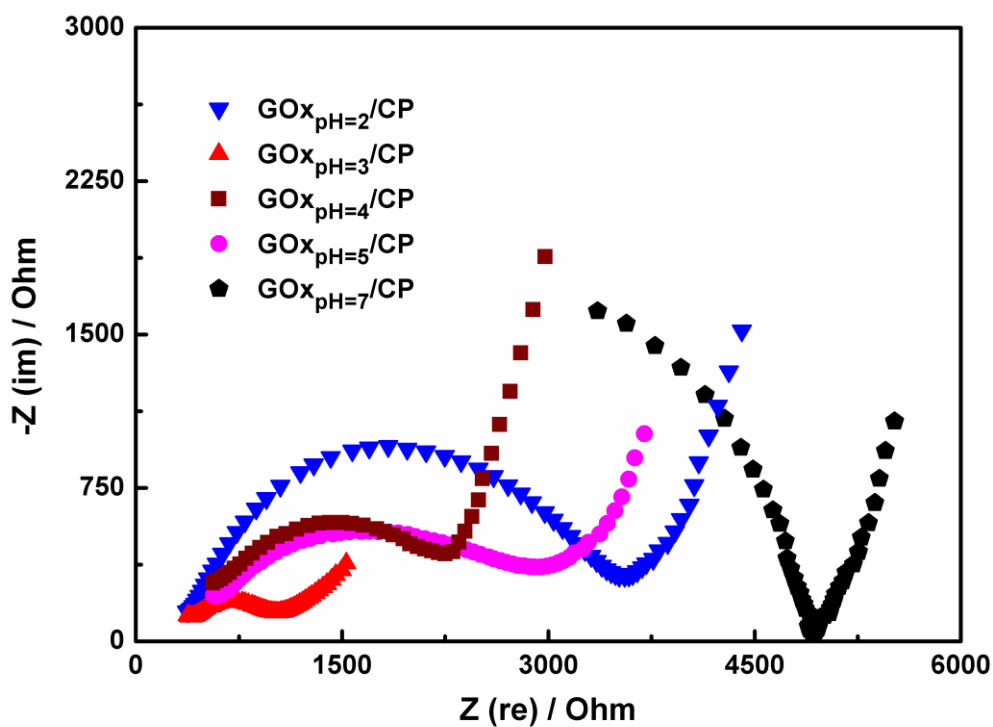


**Figure 3.** Nyquist plots of the  $GOx_{pH=2,3,4,5,7}/CP$ .

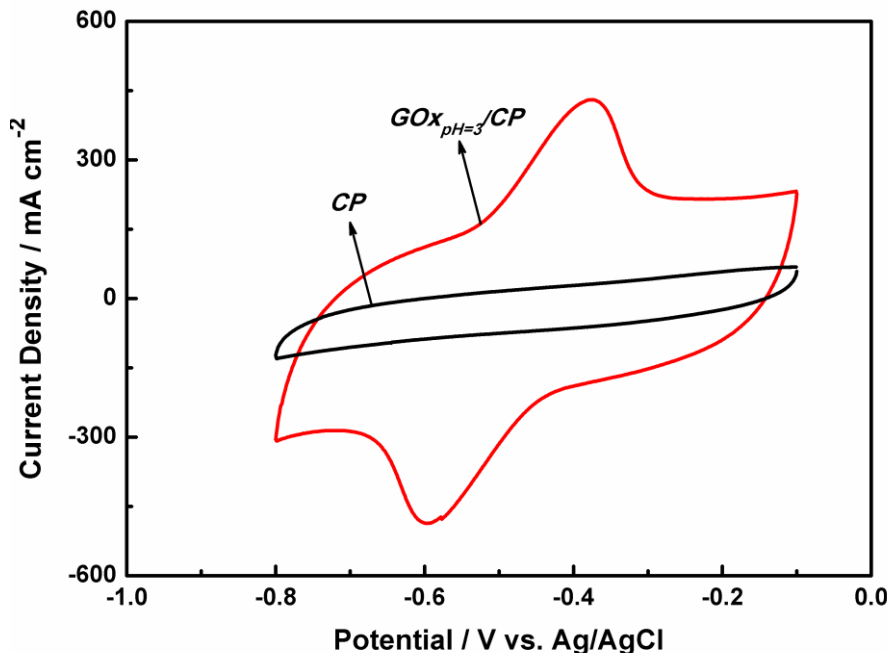


**Figure 4.** CVs of the CP and the  $\text{GOx}_{\text{pH}=3}/\text{CP}$  electrodes in Ar-saturated 0.1 M PBS.

Electrochemical impedance spectroscopy was used to determine the electron transfer resistance between the GOx and the electrodes [38, 40]. In the Nyquist plots of Figure 3, a semicircle in the high frequency region and a straight line in the low frequency region are displayed. Here, each semicircle diameter is used to estimate the interfacial electron transfer resistance ( $R_{ct}$ ) of the GOx [3, 21, 40]. Obviously, the  $R_{ct}$  of  $\text{GOx}_{\text{pH}=3}/\text{CP}$  is estimated to be minimum, indicating significantly improved electrical conductivity of  $\text{GOx}_{\text{pH}=3}/\text{CP}$  compared with that of  $\text{GOx}_{\text{pH}=2,4,5,7}/\text{CP}$ . The achievement of good electrical coupling and significantly improved electron transfer resistance of  $\text{GOx}_{\text{pH}=3}/\text{CP}$  can be attributed to the appropriate surface charge distribution and the one-step facile immobilization method of the bioanode. Therefore, we chose  $\text{GOx}_{\text{pH}=3}/\text{CP}$  as the optimal electrode in the following experiments.

The DET of  $\text{GOx}_{\text{pH}=3}/\text{CP}$  was investigated and characterized by CVs in 0.1 M PBS (pH 7.2) with a scan rate of  $10 \text{ mV s}^{-1}$ . As depicted in Figure 4, the  $\text{GOx}_{\text{pH}=3}/\text{CP}$  electrode exhibits a pair of well-defined and quasi-reversible redox peaks that originated from the reversible reaction of FAD while the CP does not show any redox peaks. This shows that there is a distinct redox peak associated with FAD within GOx, further indicating the successful achievement of DET between the GOx active center and the electrode.

### 3.3. Bioelectrocatalytic activity of $\text{GOx}_{\text{pH}=3}/\text{CP}$

The bioelectrocatalytic activity of  $\text{GOx}_{\text{pH}=3}/\text{CP}$  was investigated and characterized by CVs. During the process, the redox reactivity of FAD was measured in the  $\text{O}_2$ -free state because we intended to exclude interference by  $\text{O}_2$  on the FAD redox reaction. However, because the  $\text{GOx}_{\text{pH}=3}/\text{CP}$  is

actually used in air state while carrying out the glucose oxidation reaction at the anode of the EBC, it is necessary to investigate the influence of glucose and O<sub>2</sub> on the reactivity of GOx<sub>pH=3</sub>/CP. The following are reactions that are associated with the reaction of GOx<sub>pH=3</sub>/CP [22, 41, 42]:

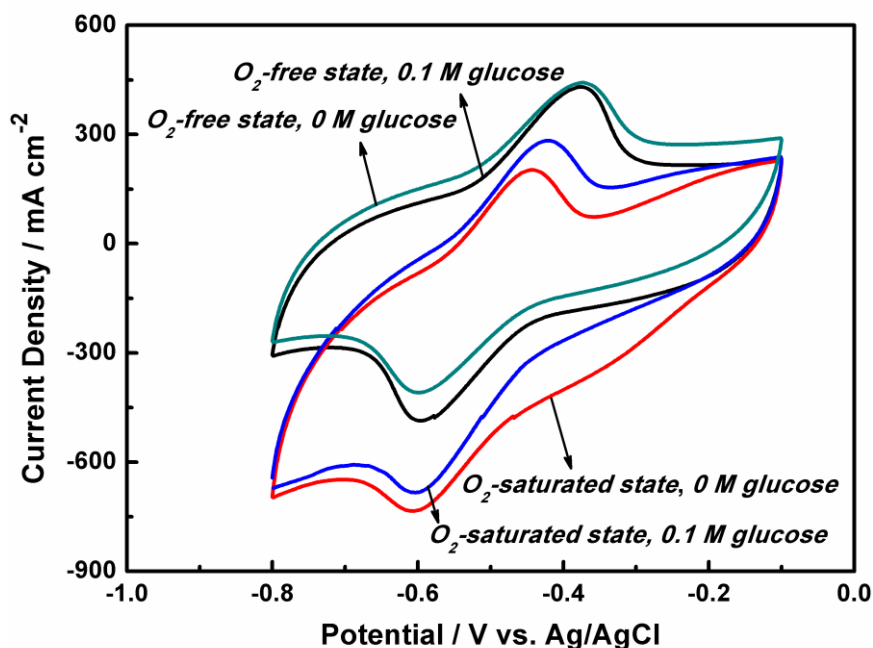
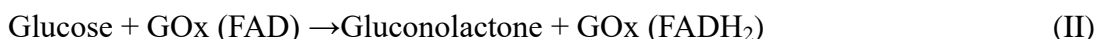


**Figure 5.** CVs of the GOx<sub>pH=3</sub>/CP in Ar-saturated PBS, O<sub>2</sub>-saturated PBS, Ar-saturated PBS containing 0.1 M glucose, and O<sub>2</sub>-saturated PBS containing 0.1 M glucose. Scan rate is 10 mV s<sup>-1</sup>, and 0.1 M PBS (pH 7.2) is used as the electrolyte.

Figure 5 shows impact of glucose on the redox reaction of FAD in an O<sub>2</sub>-free state and in air-state. For the test of the O<sub>2</sub>-free state, 0.1 M glucose was provided and the result was compared with the result of the test performed without the provision of glucose. As shown, the cathodic peak of FAD (forward reaction of reaction I) is decreased, while the anodic peak of FAD (backward reaction of reaction I) remains unchanged. This indicates that when glucose is provided, some immobilized GOx participate in the glucose oxidation (reaction II). This glucose sensitivity therefore proves our DET GOx<sub>pH=3</sub>/CP bioanode can function as a sensitive glucose sensor without any mediators.

When O<sub>2</sub> is included, the CV curve shifts downward. This could be explained if a superposition of reaction I and reaction III occurs. Since GOx is an oxygen autophagy enzyme (as shown in reaction III) and O<sub>2</sub> is a perfect electron acceptor [39], then reaction III is rapid [42]. That's to say, once GOx (FADH<sub>2</sub>) is produced in the O<sub>2</sub>-saturated state (forward reaction of reaction I), it is reduced to GOx (FAD) quickly (reaction III). Therefore, when the oxidation of GOx (FADH<sub>2</sub>) from the electrode (backward reaction of reaction I) decreases, the reduction of GOx (FAD) from the electrode (forward reaction of reaction I) increases. When 0.1 M glucose is fed to the O<sub>2</sub>-saturated electrolyte, the CV curve is shifted upward. This situation is attributed to the O<sub>2</sub>. When glucose and O<sub>2</sub> are both included,

superposition of reaction I, II and III occurs. Glucose oxidation (reaction II) produces GOx (FADH<sub>2</sub>), and this relieves the need of GOx (FADH<sub>2</sub>) provided from the electrode for O<sub>2</sub> reduction (reaction III). So the anodic peak of FAD (backward reaction of reaction 1) is increased [40, 43].

These results further demonstrate that the GOx molecules immobilized at pH 3 maintain their natural biocatalytic activities toward the substrate (glucose), again indicating that the GOx<sub>pH=3</sub>/CP prepared by this facile method can be used as a bioanode for glucose-based BFC and sensors [40].

### 3.4. $k_s$ and $K_m^{app}$ of GOx<sub>pH=3</sub>/CP

Figure 6A shows the CVs of the GOx<sub>pH=3</sub>/CP electrode in 0.1 M Ar-saturated PBS with the pH increasing from 5 to 9 at a scan rate of 10 mV s<sup>-1</sup>. The value of  $E^0$  varies linearly relatively as the pH increases with a slope nearly equal to the theoretical value of 59 mV pH<sup>-1</sup> (insert of Figure 6A), suggesting a quasi-reversible and surface-controlled electrochemical reaction with an equal number ( $n = 2$ ) [23, 25, 27, 29, 42].

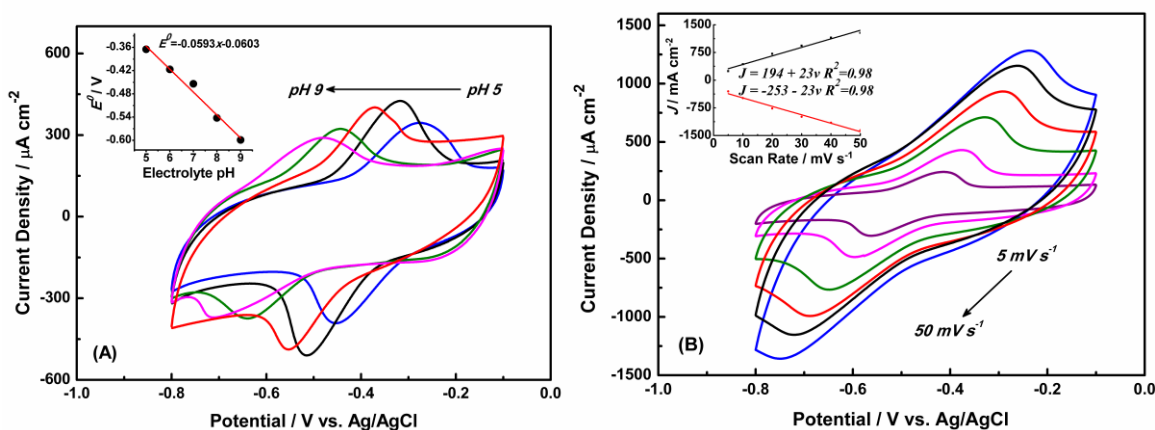


**Figure 6.** (A) CVs of the GOx<sub>pH=3</sub>/CP in Ar-saturated 0.1 M PBS with pH values of 5, 6, 7, 8 and 9. The inset is the plot of formal potential vs. pH. The scan rate is 10 mV s<sup>-1</sup>. (B) CVs of the GOx<sub>pH=3</sub>/CP at different scan rates in Ar-saturated 0.1 M PBS (pH 7.2). Inset is the relationship between the peak current and the scan rate.

Another way to probe the redox reaction of GOx<sub>pH=3</sub>/CP is to calculate the electron transfer rate constant ( $k_s$ ). As  $k_s$  increases, the electron transfer rate increases. This promotes the redox reaction of FAD within GOx.  $k_s$  can be measured by Laviron theory [27, 44],

$$k_s = mnFv/RT \quad (\text{IV})$$

where  $m$  is a constant determined by  $\Delta E_p$ ,  $n$  is the electron transfer number,  $F$  is the Faraday constant,  $v$  is the scan rate,  $R$  is the universal gas constant, and  $T$  is the temperature (room temperature).

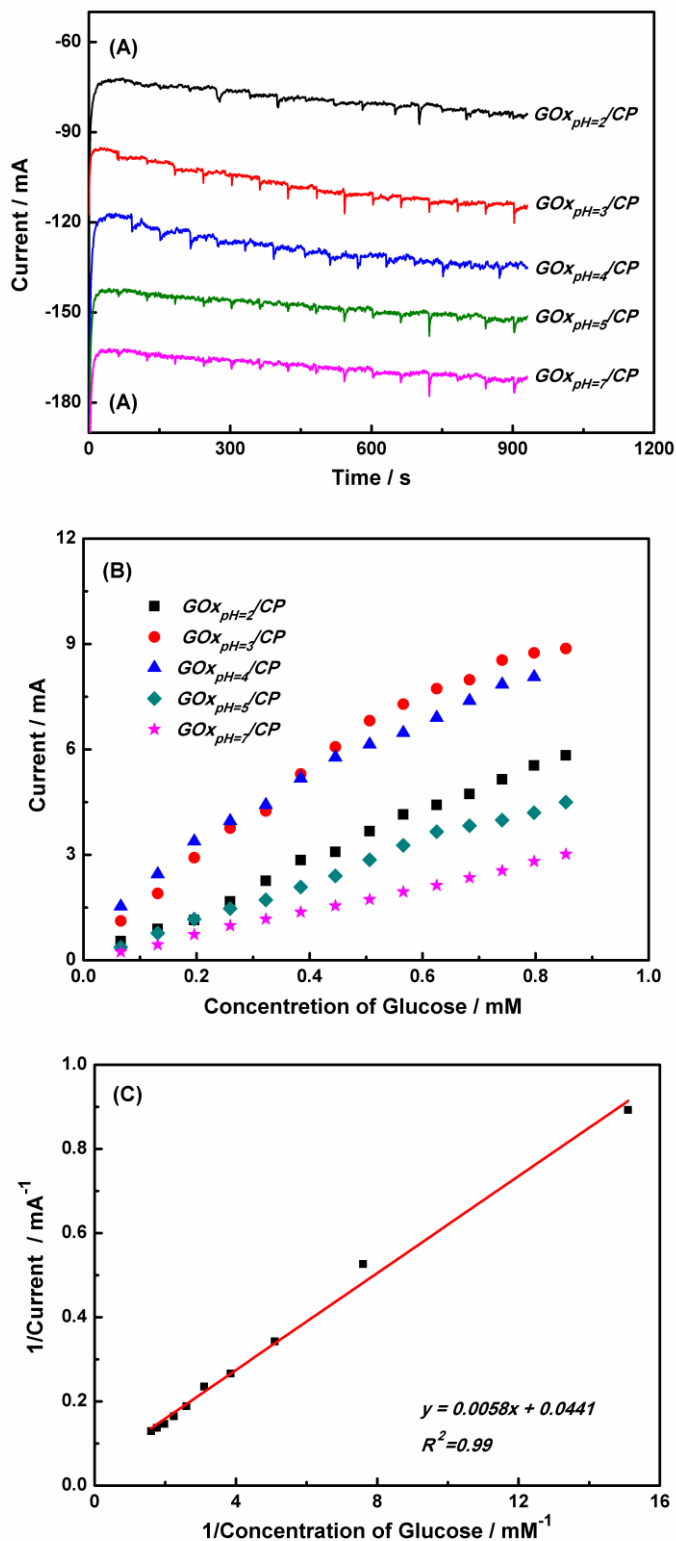


**Figure 7.** (A) Chronoamperometric  $i-t$  response of the  $GOx_{pH=x}/CP$  to glucose with various concentrations in Ar-saturated 0.1 M PBS at  $-0.46$  V. The volume of initial electrolyte is 30 mL 0.1 M PBS; inject 200  $\mu$ L 0.1 M PBS containing 10 mM glucose every time, per 60 s inject one time. The electrolyte is stirred by a magnetic stirring apparatus; the speed of rotation is 400  $r\ min^{-1}$ . (B) Plot of response current ( $\Delta i$ ) vs. concentration of glucose. (C) Lineweaver-Burk ( $1/\Delta i - 1/\text{concentration of glucose}$ ) plot for  $K_m^{app}$  determination.

CV measurements were used to determine the value of  $k_s$  for GOx<sub>pH=3</sub>/CP (Figure 6B). The calculated  $k_s$  value,  $12.08 \pm 1.0 \text{ s}^{-1}$ , is larger than the value reported for a modified GOx electrode in a conductive nanomaterial [45-49]. It indicates that the proposed fabrication method for the enzymatic modified electrode promotes DET and an increased electron transfer rate.

The small value of  $\Delta E_p$  for GOx<sub>pH=3</sub>/CP is 40 mV at a scan rate of  $1 \text{ mV s}^{-1}$  (Figure S2). This agrees well with the theoretical value, and indicates a fast electron transfer process [27]. All of the results indicate that the DET of GOx could be achieved by reducing the pH of the incubation medium during the immobilization process. The CV of GOx<sub>pH=3</sub>/CP was scanned continuously in 0.1 M PBS (pH 7.2), the voltammetric response remains almost constant even after 50 cycles (see Figure S3), indicating that the DET of GOx immobilized on the surface of CP has good stability.

As shown in the inset of Figure 6B, the redox peak current increases linearly as the potential scan rate increases from 5 to 50  $\text{mV s}^{-1}$ , further demonstrating that GOx<sub>pH=3</sub>/CP is a surface reaction-confined system [50]. Faraday's law is used to estimate the average surface concentration of electroactive GOx ( $\Gamma^*$ , in  $\text{mol cm}^{-2}$ ) in the GOx<sub>pH=3</sub>/CP electrode from CVs [51].

$$I_p = nFQv/4RT = n^2F^2A\Gamma^*v/4RT \quad (\text{V})$$

This equation can be transformed as follows [40]:

$$\Gamma^* = Q/nFA \quad (\text{VI})$$

where  $Q$  is the charge consumed in CVs,  $n$  is the electron transfer number,  $F$  is the Faraday constant, and  $A$  is the effective surface area of the electrode. The calculated  $\Gamma^*$  of the GOx<sub>pH=3</sub>/CP is  $7.80 \times 10^{-9} \text{ mol cm}^{-2}$ , which is one or two orders of magnitude larger than values reported previously [27, 43, 46, 48, 49]. This shows that the immobilized GOx incubated under acidic conditions (pH 3) has a perfect affinity to the CP and can be maintained with high catalytic activity and stability.

Amperometry was used to determine the relationship between the electrocatalytic reduction current and the glucose concentration. Figure 7A shows the chronoamperometric  $i-t$  response of the GOx<sub>pH=x</sub>/CP electrodes to glucose, where the amperometer was operated at  $-0.46\text{V}$  in 30 mL of Ar-saturated 0.1 M PBS.

The steady-state current of GOx<sub>pH=x</sub>/CP ( $x=2, 3, 4, 5,$  and  $7$ ) increases with the addition of aliquots of glucose (Figure 7B). The electrode responds rapidly to the addition of glucose. Anodic current values of the COx<sub>pH=3</sub>/CP electrode change linearly as the glucose concentration is increased from 0.01 to 0.9 mM (Figure 7C). The apparent Michaelis-Menten constant ( $K_m^{app}$ ) provides an indication of enzyme-substrate kinetics and the biological activity of the immobilized enzyme [23].  $K_M^{app}$  is determined from an Eadie-Hofstee plot using Lineweaver-Burk equation [23, 50].

$$1/I_{ss} = 1/I_{max} + K_m^{app}/(I_{max}c) \quad (\text{VII})$$

where  $I_{ss}$  is the steady-state current after the addition of substrate (glucose),  $c$  is the bulk substrate concentration, and  $I_{max}$  is the maximum current measured under saturated substrate conditions.  $K_m^{app}$  can be calculated by analyzing the slope and intercept of the plot of the reciprocals of the steady-

state current vs. glucose concentration (Figure 7C). The  $K_m^{app}$  of the immobilized GOx was calculated to be  $0.13 \pm 0.01$  mM, which is much lower than the value of 0.85 mM reported for immobilized GOx on carbon nanodots [49, 51]. It implies that the GOx immobilized by our method and the prepared electrode possesses relatively high enzymatic activity and affinity for glucose, respectively.

The apparent rate of catalysis ( $K_{cat}$ , or turnover rate constant), which represents the maximum number of substrate molecules that can be converted into products per catalytic site, is calculated from the Lineweaver-Burk plot according to the equation [45],  $I_{max} = nFAK_{cat}$ , where  $I_{max}$  is the maximum current. When  $K_m^{app}$  and  $K_{cat}$  values for the immobilized GOx are determined for different pH values

(Table S2), the optimal values are obtained at pH 3.

The electrocatalytic characteristics (such as  $k_s$ ,  $I^*$  and  $K_m^{app}$ ) of GOx-modified bioanode toward the oxidation of glucose are compared to some of the bioanodes previously reported for the electrocatalytic oxidation of glucose (Table 1).

**Table 1.** Comparison of electrocatalytic characteristics between GOx<sub>pH=3</sub>/CP electrode and other modified electrodes.

Electrode	$k_s$ (s <sup>-1</sup> )	$I^*$ (mol cm <sup>-2</sup> )	$K_m^{app}$ (mM)	Reference
GOx-CNT mat	1.71	$(3.27 \pm 0.2) \times 10^{-13}$	2.18	[46]
Nafion/GOx/Ag-Pdop@CNT/GCE	3.6	n.d.	5.46	[47]
GOx/AP/GCE	4.25	$1.23 \times 10^{-12}$	2.95	[48]
GOx-CNDs/GCE	$6.28 \pm 0.05$	$4.08 \times 10^{-11}$	$0.85 \pm 0.03$	[49]
GOx <sub>pH=3</sub> /CP	$12.08 \pm 1.00$	$7.80 \times 10^{-9}$	$0.13 \pm 0.01$	This work

### 3.5. BFC tests

Using the proposed method, glucose can be directly and bioelectrocatalytically oxidized near the redox active potential of GOx on a GOx/CP electrode via a DET reaction. This approach could be desirable for increasing the open circuit voltage (OCP) of the cell and for constructing a bioanode for use in DET-type BFCs. We used a GOX<sub>pH=x</sub>/CP enzymatic electrode as the bioanode of a glucose/air BFC. The polarization curve of the hybrid BFC, consisting of a freshly prepared GOX<sub>pH=3</sub>/CP bioanode and an air-breathing Pt cathode, reveals that the bioanode generated an OCP of 0.79 V, a maximum power density of 65  $\mu\text{W cm}^{-2}$ , and a maximum current density of 216  $\mu\text{A cm}^{-2}$  (Figure 8A). Reducing

the pH of the incubation medium enhances the current density and power density (Figure 8B), although the power density decreases when the pH is too low (i.e., pH 2). These data corroborate the kinetic results and the morphology of the immobilized GOx on the CP surface.

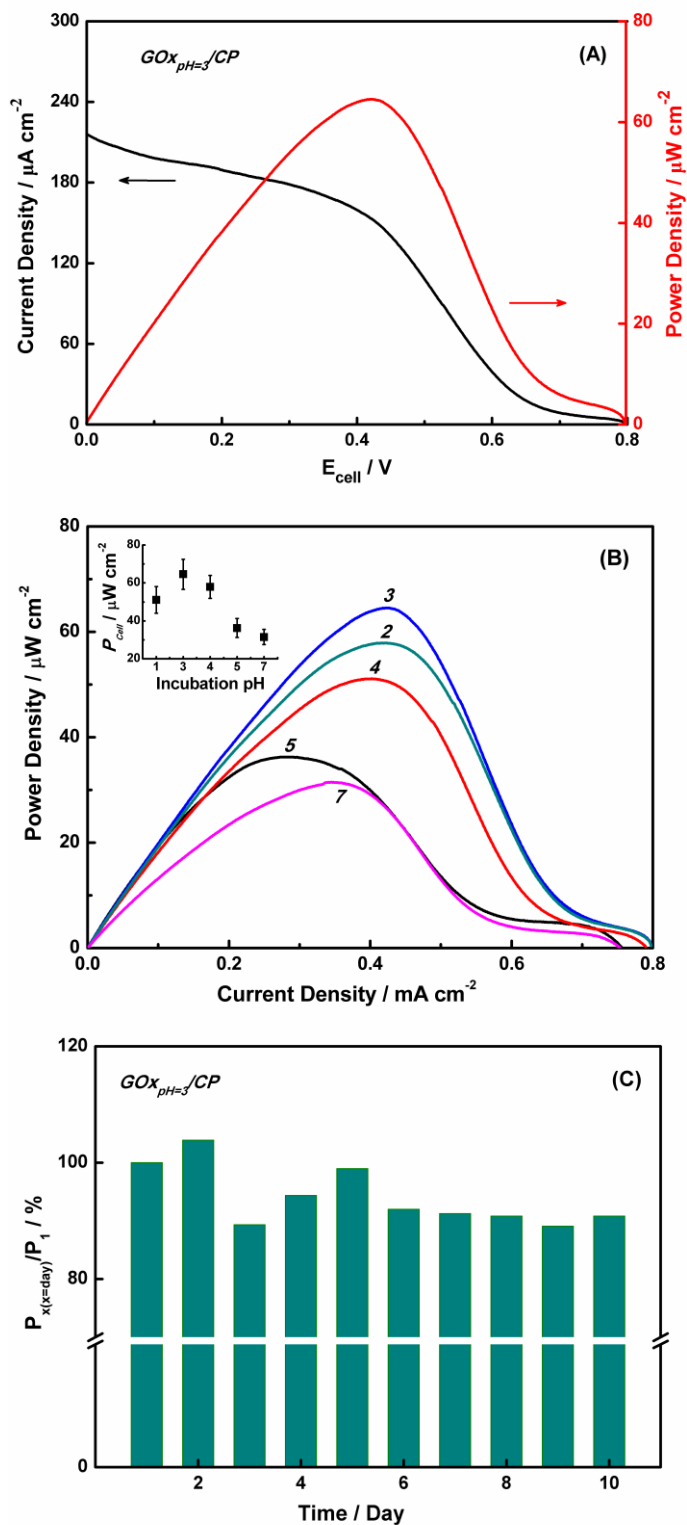


**Figure 8.** (A) The polarization curves and power outputs of the glucose BFCs:  $\text{GOx}_{\text{pH}=3}/\text{CP}$  bioanode vs. platinum foil biocathode in 30 mL 0.1 M PBS containing 0.1 M glucose and 30 mL  $\text{O}_2$ -saturated 0.1 M B-R solution, respectively. (B) Power density curves as a function of the pH. (C) Stability test of the biofuel cell ( $\text{GOx}$ , glucose//Pt,  $\text{O}_2$ ). The value of power density control (100%) corresponds to 65  $\mu\text{W cm}^{-2}$ .

Comparing our data with previous literature is difficult due to the many experimental differences. Nevertheless, the maximum power density value for the  $\text{GOx}_{\text{pH}=3}/\text{CP}$  DET system are comparable to values from recent studies employing similar GOx modified anodes and Pt cathodes [27, 52]. The maximum power density generated by the  $\text{GOx}_{\text{pH}=3}/\text{CP}$  system remained constant for 2 days at  $65 \pm 3 \mu\text{W cm}^{-2}$  and retained 91% of its initial value after 10 days (Figure 8C). These results

demonstrate good stability of the bioelectrode over this period.

Considering all of the electrochemical data and BFCs test results, we conclude that the  $\text{GOx}_{\text{pH}=3}/\text{CP}$  bioanode is very easy to prepare using our method, and that the electrocatalyst permits efficient DET between GOx and the electrode. The proposed method is highly recommended as a potential platform for use in advanced bioelectronic device applications.

#### 4. CONCLUSIONS

A simple and convenient biomolecule immobilization approach, which does not employ specific reagents or involve a complex multistep process, has been proposed for the fabrication of a GOx modified electrode with DET for glucose BFCs or biosensors. In this approach, GOx is incorporated directly into CP by adjusting the incubation medium to a lower pH (i.e., pH 3) during the immobilization process. The immobilized GOx was capable of electrons transfer with the electrode directly and efficiently due to the electron relaying function of CP. In addition to describing a versatile platform for biomolecule immobilization, this work provides a new insight into the preparation of other enzymes or biomolecules for potential applications in many fields, such as BFCs, biosensing, and other bioelectrochemical devices.

#### SUPPORTING INFORMATION:

(1) The morphology of the bare CP and pretreated CP.

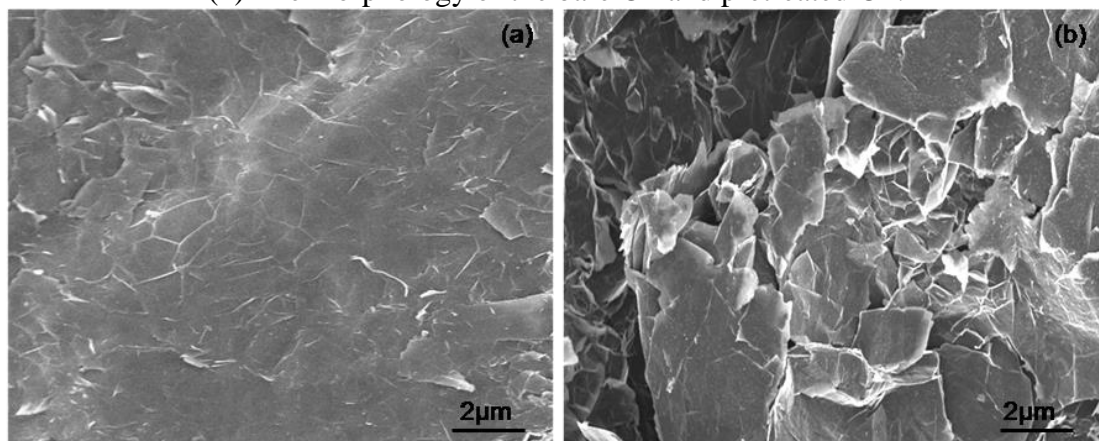


**Figure S1.** SEM images of (a) bare CP and (b) pretreated CP.

(2) The zeta potentials of the pretreated CP in the GOx solution at various pH values.

**Table S1.** Zeta potentials of the pretreated CP in the GOx solution at various pH values.

Incubation pH of GOx	2	3	4	5	7
Zeta potential /mV	$-8.5 \pm 5$	$-6.7 \pm 2$	$-5.2 \pm 2$	$-4.3 \pm 4$	$-2.2 \pm 2$

(3) The peak-peak separation of  $\text{GOx}_{\text{pH}=3}/\text{CP}$ .

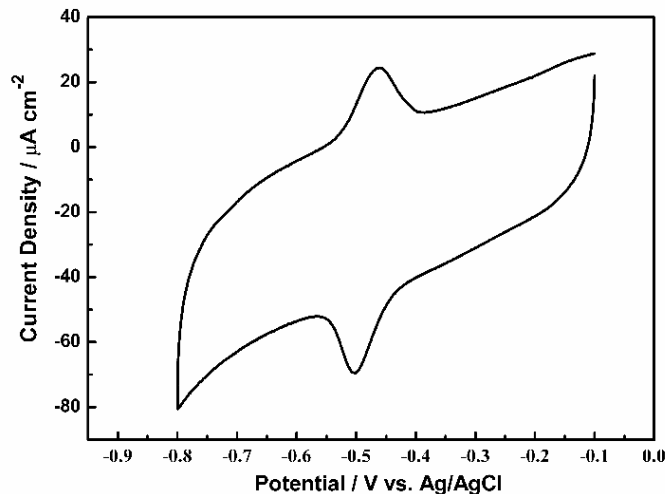


**Figure S2.** CVs obtained at  $\text{GOx}_{\text{pH}=3}/\text{CP}$  operated in 20 mL Ar-saturated 0.1 M PBS contained 0.1 M  $\beta$ -D-glucose stock solution, scan rate:  $1 \text{ mV s}^{-1}$ .

(4) The stability of  $\text{GOx}_{\text{pH}=3}/\text{CP}$  electrode.

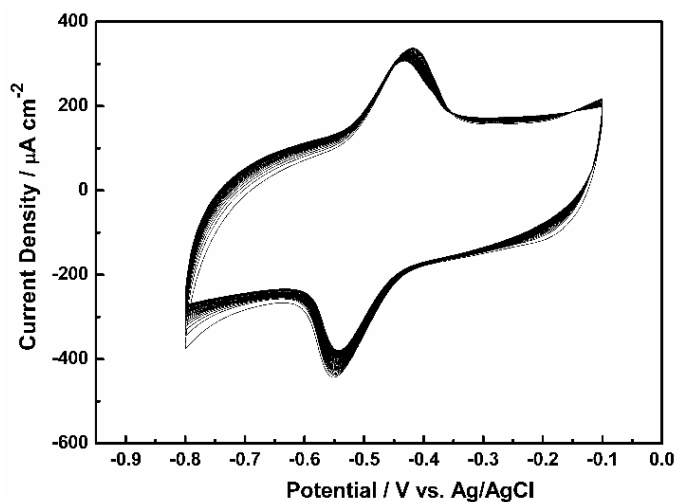


**Figure S3.** CVs obtained at  $\text{GOx}_{\text{pH}=3}/\text{CP}$  operated in 20 ml Ar-saturated 0.1 M PBS contained 0.1 M  $\beta$ -D-glucose stock solution, scan rate:  $10 \text{ mV s}^{-1}$ , circles: 50.

(5) The  $K_m^{app}$  and  $K_{cat}$  of different GOx immobilized at various pH values

**Table S2.** Apparent Steady-State Michaelis-Menten constant  $K_m^{app}$  and catalytic efficiencies  $K_{cat}$  of immobilized GOx at different pH values.

pH	2	3	4	5	7
$K_m^{app}$ / mM	0.70±0.04	0.13±0.01	0.39±0.03	0.54±0.05	1.45±0.15
$K_{cat}$ / $\times 10^{-12}$ M cm <sup>-2</sup> s <sup>-1</sup>	69.4±4.2	117.6±9.4	53.8±4.3	29.1±2.6	9.6±1.0

## ACKNOWLEDGMENTS

Financial support for this work was provided by National Natural Science Foundation of China through grant 81301345 and 61402486.

## References

1. A. Navaee and A. Salimi, *J. Mater. Chem. A*, 3 (2015) 7623.
2. D. M. Eby, K. Artyushkova, A. K. Paravastu and G. R. Johnson, *J. Mater. Chem.*, 22 (2012) 9875.
3. X. Kang, J. Wang, H. Wu, I. A. Aksay, J. Liu and Y. Lin, *Biosens. Bioelectron.*, 25 (2009) 901.
4. C. Gutierrez-Sanchez, M. Pita, C. Vaz-Dominguez, S. Shleev and A. L. De Lacey, *J. Am. Chem. Soc.*, 134 (2012) 17212.
5. A. Zebda, C. Gondran, A. Le Goff, M. Holzinger, P. Cinquin and S. Cosnier, *Nat. Commun.*, 2 (2011) 370.
6. C. Cai and J. Chen, *Anal. Biochem.*, 332 (2004) 75.
7. M. R. Karim, Y. Ikeda, T. Ide, S. Sugimoto, K. Toda, Y. Kitamura, T. Ihara, T. Matsui, T. Taniguchi and M. Koinuma, *New J. Chem.*, 38 (2014) 2120.
8. D. Brugger, I. Krondorfer, C. Shelswell, B. Huber-Dittes, D. Haltrich and C. K. Peterbauer, *Plos One*, 9 (2014) e109242.
9. X. Du, Z. Miao, D. Zhang, Y. Fang, M. Ma and Q. Chen, *Biosens. Bioelectron.*, 62 (2014) 73.
10. O. Yehezkeli, R. Tel-Vered, S. Raichlin and I. Willner, *ACS Nano*, 5 (2011) 2385.
11. J. T. Holland, C. Lau, S. Brozik, P. Atanassov and S. Banta, *J. Am. Chem. Soc.*, 133 (2011) 19262.
12. M. Ahmad, C. F. Pan, Z. X. Luo and J. Zhu, *J. Phys. Chem. C*, 114 (2010) 9308.
13. K. Tao, C. Yang, Y. Yiping, Z. Kun, W. Zhenxing and W. Xiaoping, *Sensor Actuat. B-Chem.*, 38 (2009) 344.
14. M. Magro, G. Sinigaglia, L. Nodari, J. Tucek, K. Polakova, Z. Marusak, S. Cardillo, G. Salviulo, U. Russo, R. Stevanato, R. Zboril and F. Vianello, *Acta Biomater.*, 8 (2012) 2068.
15. H. W. Yang, M. Y. Hua, S. L. Chen and R. Y. Tsai, *Biosens. Bioelectron.*, 41 (2013) 172.
16. L. Sasso, S. Suei, L. Domigan, J. Healy, V. Nock, M. A. K. Williams and J. A. Gerrard, *Nanoscale*, 6 (2014) 1629.
17. Y. Y. Yu, Z. G. Chen, S. J. He, B. B. Zhang, X. C. Li, M and C. Yao, *Biosens. Bioelectron.*, 52 (2014) 147.
18. D. Y. Zhai, B. R. Liu, Y. Shi, L. J. Pan, Y. Q. Wang, W. B. Li, R. Zhang and G. H. Yu, *ACS Nano*, 7 (2013) 3540.
19. C. Charan and V. K. Shahi, *J. Appl. Electrochem.*, 44 (2014) 953.
20. Y. L. Wang, L. Liu, M. G. Li, S. D. Xu and F. Gao, *Biosens. Bioelectron.*, 30 (2011) 107.
21. M. Zhang, A. Smith and W. Gorski, *Anal. Chem.* 76 (2004) 5045.
22. F. Giroud and S. D. Minteer, *Electrochem. Commun.*, 34 (2013) 157.
23. M. Zhao, Y. Gao, J. Sun and F. Gao, *Anal. Chem.*, 87 (2015) 2615.
24. K. Hyun, S. W. Han, W.-G. Koh and Y. Kwon, *Int. J. Hydrogen Ener.*, 40 (2015) 2199.

25. Y. Zhang, M. Chu, L. Yang, Y. Tan, W. Deng, M. Ma, X. Su and Q. Xie, *ACS Appl. Mater. Inte.*, 6 (2014) 12808.
26. H. U. Lee, H. Y. Yoo, T. Lkhagvasuren, Y. S. Song, C. Park, J. Kim and S. W. Kim, *Biosens. Bioelectron.*, 42 (2013) 342.
27. K. P. Prasad, Y. Chen and P. Chen, *ACS Appl. Mater. Inte.*, 6 (2014) 3387.
28. K. Zhang, X. Duan, X. Zhu, D. Hu, J. Xu, L. Lu, H. Sun and L. Dong, *Synthetic Met.*, 195 (2014) 36.
29. Q. Liu, X. Lu, J. Li, X. Yao and J. Li, *Biosens. Bioelectron.*, 2 (2007) 3203.
30. E. Rozniecka, M. –N. Jonsson, J. W. Sobczak and M. Opallo, *Electrochim. Acta*, 56 (2011) 8739.
31. B. Astinchap, R. Moradian, A. Ardu, C. Cannas and G. Varvaro, *Chem. Mater.*, 24 (2012) 3393.
32. N. S. Aquino, T. S. Almeida, L. M. Palma, S. D. Minter and A. R. de Andrade, *J. Power Sources*, 259 (2014) 25.
33. A. D. Chowdhury, R. Gangopadhyay and A. De, *Sensor Actuat. B-Chem.*, 190 (2014) 348.
34. R. Tosaka, H. Yamamoto, I. Ohdomari and T. Watanabe, *Langmuir*, 26 (2010) 9950.
35. S. Hudson, J. Cooney and E. Magner, *Angewandte Chemie*, 47 (2008) 8582.
36. C. Thörn, D. B. R. K. G. Udatha, H. Zhou, P. Christakopoulos, E. Topakas and L. Olsson, *J. Mol. Catal. B-Enzym.*, 93 (2013) 65.
37. N. Stănciuc, I. Aprodu, E. Ionitǎ, G. Bahrim and G. Rǎpeanu, *Spectrochim. Acta A*, 147 (2015) 43.
38. R. Montes, J. Bartrolí, M. Baeza and F. Céspedes, *Microchem. J.*, 119 (2015) 66.
39. S. B. Bankar, M. V. Bule, R. S. Singhal and L. Ananthanarayan, *Biotechnol. Adv.*, 27 (2009) 489.
40. J. Chen, R. Zhu, J. Huang, M. Zhang, H. Liu, M. Sun, L. Wang and Y. Song, *Analyst*, 140 (2015) 5578.
41. K. P. Prasad, Y. Chen and P. Chen, *ACS Appl. Mater. Inte.*, 6 (2014) 3387.
42. A. A. Sehat, A. A. Khodadadi, F. Shemirani and Y. Mortazavi, *Int. J. Electrochem. Sc.*, 10 (2015) 272.
43. Y. F. Gao, T. Yang, X. L. Yang, Y. S. Zhang, B. L. Xiao, J. Hong, N. Sheibani, H. Ghourchian, T. Hong and -M. A. A. Moosavi, *Biosens. Bioelectron.*, 60 (2014) 30.
44. S. Liu and H. Ju, *Biosens. Bioelectron.*, 19 (2003) 177.
45. M. Mathew and N. Sandhyarani, *Anal. Biochem.*, 459 (2014) 31.
46. J. Ryu, H. Kim, S. Lee, H. T. Hahn and D. Lashmore, *J. Nanosci. Nanotechno.*, 10 (2010) 941.
47. Y. L. Wang, L. Liu, M. G. Li, S. D. Xu and F. Gao, *Biosens. Bioelectron.*, 30 (2011) 107.
48. Z. Nasri and E. Shams, *Electrochim. Acta*, 112 (2012) 640.
49. M. Zhao, Y. Gao, J. Y. Sun and F. Gao, *Anal. Chem.*, 87 (2015) 2615.
50. X. Kang, J. Wang, H. Wu, I. A. Aksay, J. Liu and Y. Lin, *Biosens. Bioelectron.*, 25 (2009) 901.
51. S. Zhu, H. Li, W. Niu and G. Xu, *Biosens. Bioelectron.*, 25 (2009) 940.
52. C. Hou, D. Yang, B. Liang and A. Liu, *Anal. Chem.*, 86 (2014) 6057.